Seasonal variation and latitudinal distribution of the instability of two-level quasi-geostrophic waves in horizontal shear

By CHUNG-MUH TANG, *Department of Geology and Geophysics, Yale University, New Haven, Conn. 06520, USA*

(Manuscript received September 28; revised version December 15, 1972)

ABSTRACT

The instability of a simplified, combined baroclinic-barotropic, two-level quasi-geostrophic model is investigated. The results are applied to the observed mean zonal wind, which varies with season and latitude, by approximating the sphericity of the earth by infinite tangent β-planes. Maximum instability is found to exist in winter at about 37° N, for zonal wave number 7, changing to zonal wave number 6 in higher middle latitudes and to lower zonal wave numbers in polar latitudes. The latitudinal and spectral bands of instability shrink gradually from winter through spring, reach a minimum in summer, and gradually widen in fall.

1. Introduction

The combined baroclinic-barotropic stability problem is indeed very difficult due to the non-separability of the governing differential equation. Attention has been focused on solving the baroclinic problem and barotropic problem separately in order to avoid the mathematical difficulty and to understand each distinct dynamical process. However, because the real atmosphere is both baroclinic and barotropic, a realistic model should include both effects. Therefore, in the past, numerical methods were sought to solve the combined baroclinic-barotropic stability problem (cf. Pedlosky, 1964; Brown 1969*a*, *b*). In the few analytical studies of this problem, such as by Pedlosky (1965) and McIntyre (1970), the component of the basic zonal flow which contained the horizontal shear was considered to be a small departure from the component of the basic zonal flow which is uniform in the meridional direction.

It is apparent that some kind of approximation is needed to make the mathematical problem separable and yet allow both the influence of the observed vertical shear of the mean zonal flow and the observed horizontal shear of the mean zonal flow on the disturbance. To this end, we shall here assume that we are dealing with waves of comparatively large meridional extent so that we can ignore the second derivative of the perturbation stream function in the meridional direction in evaluating the perturbation vorticity. This approximation was used with good results by Saltzman & Vernekar (1968) in the parameterization of the large-scale transient eddy flux of relative angular momentum. Furthermore, as shown in the Appendix, the stability results obtained with this approximation are almost identical with those of Pedlosky (1964) who did not assume the meridional form of the perturbation.

In this study we shall use a β-plane approximation in the two-level quasi-geostrophic model and we shall study not only the normal mode solution, but also the *characteristic waves* as defined by Holmboe (1966, 1967). By applying each β-plane locally at each latitude circle using the observed mean zonal flow (Oort & Rasmusson, 1971), we obtain the seasonal variation and the latitudinal distribution of the growth rate and phase speed of the two-level quasi-geostrophic modes. A similar method was used by Phillips (1954), Fleagle (1957) and Árnason (1961, 1963), but these authors did not attempt to include the effects of horizontal shear of the mean zonal flow.

2. The normal modes

The model considered is the traditional two-level model (cf. Phillips, 1954) with the quasi-geostrophic vorticity equations applied at level 1 ($p_1 = 250$ mb) and level 3 ($p_3 = 750$ mb), and the adiabatic equation applied at level 2 ($p_2 = 500$ mb). With the boundary conditions that $\omega' = 0$ at 0 and 1 000 mb, the linearized governing equations are

$$\left.\begin{aligned}
&\left(\frac{\partial}{\partial t} + \bar{u}_1 \frac{\partial}{\partial x}\right)\nabla^2 \psi_1' + \left(\beta - \frac{\partial^2 \bar{u}_1}{\partial y^2}\right)\frac{\partial \psi_1'}{\partial x} = \frac{f}{p_2}\,\omega_2' \\
&\left(\frac{\partial}{\partial t} + \bar{u}_3 \frac{\partial}{\partial x}\right)\nabla^2 \psi_3' + \left(\beta - \frac{\partial^2 \bar{u}_3}{\partial y^2}\right) \\
&\qquad\times \frac{\partial \psi_3'}{\partial x} = -\frac{f}{p_2}\,\omega_2' \\
&\left(\frac{\partial}{\partial t} + \bar{u}_2 \frac{\partial}{\partial x}\right)(\psi_1' - \psi_3') - (\bar{u}_1 - \bar{u}_3) \\
&\qquad\times \frac{\partial \psi_2'}{\partial x} - \frac{Sp_2}{f}\,\omega_2' = 0
\end{aligned}\right\} \tag{1}$$

where ψ denotes the stream function, ω denotes dp/dt, t is time, x is distance eastward, y is distance northward, ∇^2 is the Laplacian operator ($= \partial^2/\partial x^2 + \partial^2/\partial y^2$), $\bar{u}$ is the mean zonal wind, f is the Coriolis parameter at a reference latitude, β is the Rossby parameter ($= df/dy$), S is the static stability (assumed to be constant), and the prime denotes a deviation from the zonal average.

Eliminating ω_2' in (1) and ignoring $\partial^2\psi'/\partial y^2$, we obtain

$$\left.\begin{aligned}
&\left(\frac{\partial}{\partial t} + \bar{u}_1 \frac{\partial}{\partial x}\right)\left[\frac{\partial^2 \psi_1'}{\partial x^2} - \frac{f^2}{Sp_2^2}(\psi_1' - \psi_3')\right] \\
&\qquad + \left[\beta - \frac{\partial^2 \bar{u}_1}{\partial y^2} + \frac{f^2}{Sp_2^2}(\bar{u}_1 - \bar{u}_3)\right]\frac{\partial \psi_1'}{\partial x} = 0 \\
&\left(\frac{\partial}{\partial t} + \bar{u}_3 \frac{\partial}{\partial x}\right)\left[\frac{\partial^2 \psi_3'}{\partial x^2} + \frac{f^2}{Sp_2^2}(\psi_1' - \psi_3')\right] \\
&\qquad + \left[\beta - \frac{\partial^2 \bar{u}_3}{\partial y^2} - \frac{f^2}{Sp_2^2}(\bar{u}_1 - \bar{u}_3)\right]\frac{\partial \psi_3'}{\partial x} = 0
\end{aligned}\right\} \tag{2}$$

Substitution of the normal mode solution

$$\psi_1' = \hat{\Psi}_1 e^{ik(x-ct)} \tag{3a}$$

$$\psi_3' = \hat{\Psi}_3 e^{ik(x-ct)} \tag{3b}$$

into (2) yields

$$c = c_r + ic_i \tag{4}$$

where

$$c_r = \bar{u}_2 - \frac{1}{2k^2}\left(\frac{2+\lambda}{1+\lambda}\right)\left(\beta - \frac{\partial^2 \bar{u}_2}{\partial y^2}\right) \tag{5a}$$

$$c_i = \left\{\lambda^2\left[\left(\bar{u}_T + \frac{1}{2k^2}\frac{\partial^2 \bar{u}_T}{\partial y^2}\right)^2 - \frac{1}{4k^4}\left(\beta - \frac{\partial^2 \bar{u}_2}{\partial y^2}\right)^2\right] - \left[\bar{u}_T + \frac{2+\lambda}{2k^2}\frac{\partial^2 \bar{u}_T}{\partial y^2}\right]^2\right\} \Big/ (1+\lambda) \tag{5b}$$

with the definitions,

$$\bar{u}_2 = (\bar{u}_1 + \bar{u}_3)/2 \tag{6a}$$

$$\bar{u}_T = (\bar{u}_1 - \bar{u}_3)/2 \tag{6b}$$

$$\lambda = 2f^2/Sp_2^2 k^2 \tag{6c}$$

We note that c_r and c_i are both functions of y. In the Appendix we show that the stability criterion implied by (5b) is almost identical to that obtained numerically by Pedlosky (1964).

3. The characteristic waves

To investigate the time-dependent structure of the unstable waves let us assume that ψ_1' and ψ_3' are of the spatial form $exp\ (ikx)$. Using (6c), we obtain from (2):

$$\left.\begin{aligned}
&\left(\frac{\partial}{\partial t} + \bar{u}_1 \frac{\partial}{\partial x}\right)\left[-\left(1 + \frac{\lambda}{2}\right)\psi_1' + \frac{\lambda}{2}\psi_3'\right] \\
&\qquad + \left[\frac{1}{k^2}\left(\beta - \frac{\partial^2 \bar{u}_1}{\partial y^2}\right) + \frac{\lambda}{2}(\bar{u}_1 - \bar{u}_3)\right]\frac{\partial \psi_1'}{\partial x} = 0 \\
&\left(\frac{\partial}{\partial t} + \bar{u}_3 \frac{\partial}{\partial x}\right)\left[-\left(1 + \frac{\lambda}{2}\right)\psi_3' + \frac{\lambda}{2}\psi_1'\right] \\
&\qquad + \left[\frac{1}{k^2}\left(\beta - \frac{\partial^2 \bar{u}_3}{\partial y^2}\right) - \frac{\lambda}{2}(\bar{u}_1 - \bar{u}_3)\right]\frac{\partial \psi_3'}{\partial x} = 0
\end{aligned}\right\} \tag{7}$$

With some manipulation, and using (6a) and (6b), we get from (7),

$$\left.\begin{aligned}(1+\lambda)\frac{\delta\psi_1'}{\delta t} &= -\left(\bar{u}_T+\frac{2+\lambda}{2k^2}\frac{\partial^2\bar{u}_T}{\partial y^2}\right)\frac{\partial\psi_1'}{\partial x}\\&\quad+\lambda\left[\bar{u}_T+\frac{1}{2k^2}\left(\beta-\frac{\partial^2\bar{u}_2}{\partial y^2}+\frac{\partial^2\bar{u}_T}{\partial y^2}\right)\right]\frac{\partial\psi_3'}{\partial x}\\(1+\lambda)\frac{\delta\psi_3'}{\delta t} &= \left(\bar{u}_T+\frac{2+\lambda}{2k^2}\frac{\partial^2\bar{u}_T}{\partial y^2}\right)\frac{\partial\psi_3'}{\partial x}\\&\quad-\lambda\left[\bar{u}_T-\frac{1}{2k^2}\left(\beta-\frac{\partial^2\bar{u}_2}{\partial y^2}-\frac{\partial^2\bar{u}_T}{\partial y^2}\right)\right]\frac{\partial\psi_1'}{\partial x}\end{aligned}\right\}\quad(8)$$

where

$$\frac{\delta}{\delta t}=\frac{\partial}{\partial t}+c_r\frac{\partial}{\partial x}\quad(9)$$

$\delta/\delta t$ is the local change in a frame of reference which moves with the speed c_r given by (5a). Let us consider a wave of the form

$$\left.\begin{aligned}\psi_1' &= \Psi_1\sin(kx+\theta_1)=X_1\sin kx+Y_1\cos kx\\&\qquad(X_{1,3}=\Psi_{1,3}\cos\theta_{1,3})\\\psi_3' &= \Psi_3\sin(kx-\theta_3)=X_3\sin kx-Y_3\cos kx\\&\qquad(Y_{1,3}=\Psi_{1,3}\sin\theta_{1,3})\end{aligned}\right\}\quad(10)$$

Substituting (10) into (8), we obtain

$$\left.\begin{aligned}(1+\lambda)\frac{\delta X_1}{\delta t} &= k\left[\bar{u}_T+\frac{2+\lambda}{2k^2}\frac{\partial^2\bar{u}_T}{\partial y^2}\right]Y_1\\&\quad+k\lambda\left[\bar{u}_T+\frac{1}{2k^2}\left(\beta-\frac{\partial^2\bar{u}_2}{\partial y^2}+\frac{\partial^2\bar{u}_T}{\partial y^2}\right)\right]Y_3\\(1+\lambda)\frac{\delta Y_1}{\delta t} &= -k\left[\bar{u}_T+\frac{2+\lambda}{2k^2}\frac{\partial^2\bar{u}_T}{\partial y^2}\right]X_1\\&\quad+k\lambda\left[\bar{u}_T+\frac{1}{2k^2}\left(\beta-\frac{\partial^2\bar{u}_2}{\partial y^2}+\frac{\partial^2\bar{u}_T}{\partial y^2}\right)\right]X_3\\(1+\lambda)\frac{\delta X_3}{\delta t} &= k\left[\bar{u}_T+\frac{2+\lambda}{2k^2}\frac{\partial^2\bar{u}_T}{\partial y^2}\right]Y_3\\&\quad+k\lambda\left[\bar{u}_T-\frac{1}{2k^2}\left(\beta-\frac{\partial^2\bar{u}_2}{\partial y^2}-\frac{\partial^2\bar{u}_T}{\partial y^2}\right)\right]Y_1\\(1+\lambda)\frac{\delta Y_3}{\delta t} &= -k\left[\bar{u}_T+\frac{2+\lambda}{2k^2}\frac{\partial^2\bar{u}_T}{\partial y^2}\right]X_3\\&\quad+k\lambda\left[\bar{u}_T-\frac{1}{2k^2}\left(\beta-\frac{\partial^2\bar{u}_2}{\partial y^2}-\frac{\partial^2\bar{u}_T}{\partial y^2}\right)\right]X_1\end{aligned}\right\}\quad(11)$$

At the initial time $t=0$, for a given y, let us select the origin $x=0$ such that $\theta_1=\theta_3=\theta$, and the amplitude ratio, Ψ_1/Ψ_3, such that

$$\frac{\Psi_1}{\Psi_3}=\left[\frac{\bar{u}_T+\dfrac{1}{2k^2}\left(\beta-\dfrac{\partial^2\bar{u}_2}{\partial y^2}+\dfrac{\partial^2\bar{u}_T}{\partial y^2}\right)}{\bar{u}_T-\dfrac{1}{2k^2}\left(\beta-\dfrac{\partial^2\bar{u}_2}{\partial y^2}-\dfrac{\partial^2\bar{u}_T}{\partial y^2}\right)}\right]^{\frac{1}{2}}\quad(12)$$

Then for a given y at $t=0$ we have

$$\left.\begin{aligned}\frac{(1+\lambda)}{Y_1}\frac{\delta X_1}{\delta t} &= \frac{(1+\lambda)}{Y_3}\frac{\delta X_3}{\delta t}\\&=a+b\\\frac{(1+\lambda)}{X_1}\frac{\delta Y_1}{\delta t} &= \frac{(1+\lambda)}{X_3}\frac{\delta Y_3}{\delta t}\\&=a-b\end{aligned}\quad(\theta_1=\theta_3=\theta,\ t=0)\right\}\quad(13)$$

where

$$\left.\begin{aligned}a &= k\lambda\left[\left(\bar{u}_T+\frac{1}{2k^2}\frac{\partial^2\bar{u}_T}{\partial y^2}\right)^2-\frac{1}{4k^4}\left(\beta-\frac{\partial^2\bar{u}_2}{\partial y^2}\right)^2\right]^{\frac{1}{2}}\\b &= k\left[\bar{u}_T+\frac{2+\lambda}{2k^2}\frac{\partial^2\bar{u}_T}{\partial y^2}\right]\end{aligned}\right\}\quad(14)$$

The results given in (12), (13) and (14) also apply to arbitrary y, but the coordinate x changes with y. Repeated differentiations of (11), with (13) applied at $t=0$, gives

$$\left.\begin{aligned}\frac{1}{Y_1}\frac{\delta^{2n-1}}{\delta t^{2n-1}}X_1 &= \frac{1}{Y_3}\frac{\delta^{2n-1}}{\delta t^{2n-1}}X_3\\&=\frac{(a+b)^n(a-b)^{n-1}}{(1+\lambda)^{2n-1}}\\\frac{1}{X_1}\frac{\delta^{2n-1}}{\delta t^{2n-1}}Y_1 &= \frac{1}{X_3}\frac{\delta^{2n-1}}{\delta t^{2n-1}}Y_3\\&=\frac{(a-b)^n(a+b)^{n-1}}{(1+\lambda)^{2n-1}}\end{aligned}\right\}\quad(15)$$

$$\left.\begin{aligned}\frac{1}{X_1}\frac{\delta^{2n}}{\delta t^{2n}}X_1 &= \frac{1}{X_3}\frac{\delta^{2n}}{\delta t^{2n}}X_3=\frac{(a+b)^n(a-b)^n}{(1+\lambda)^{2n}}\\\frac{1}{Y_1}\frac{\delta^{2n}}{\delta t^{2n}}Y_1 &= \frac{1}{Y_3}\frac{\delta^{2n}}{\delta t^{2n}}Y_3=\frac{(a+b)^n(a-b)^n}{(1+\lambda)^{2n}}\end{aligned}\right\}\quad(16)$$

where $n = 1, 2, 3...$ By Taylor series expansion we have

$$\left.\begin{aligned} X_{1,3}(y,t) &= X_{1,3}(y,0) + \left(\frac{\delta X_{1,3}}{\delta t}\right)_0 t \\ &\quad + \frac{1}{2!}\left(\frac{\delta^2 X_{1,3}}{\delta t^2}\right)_0 t^2 + \frac{1}{3!}\left(\frac{\delta^3 X_{1,3}}{\delta t^3}\right)_0 t^3 + \dots \\ Y_{1,3}(y,t) &= Y_{1,3}(y,0) + \left(\frac{\delta Y_{1,3}}{\delta t}\right)_0 t \\ &\quad + \frac{1}{2!}\left(\frac{\delta^2 Y_{1,3}}{\delta t^2}\right)_0 t^2 + \frac{1}{3!}\left(\frac{\delta^3 Y_{1,3}}{\delta t^3}\right)_0 t^3 + \dots \end{aligned}\right\} \quad (17)$$

where the subscript zero denotes $t = 0$. Substitution of (15) and (16) into (17) gives

$$\left.\begin{aligned} X_{1,3}(y,t) &= \sqrt{\frac{a+b}{a-b}} \sinh\left[\frac{\sqrt{a^2-b^2}}{1+\lambda} t\right] \\ &\quad \times Y_{1,3}(y,0) + \cosh\left[\frac{\sqrt{a^2-b^2}}{1+\lambda} t\right] X_{1,3}(y,0) \\ Y_{1,3}(y,t) &= \sqrt{\frac{a-b}{a+b}} \sinh\left[\frac{\sqrt{a^2-b^2}}{1+\lambda} t\right] \\ &\quad \times X_{1,3}(y,0) + \cosh\left[\frac{\sqrt{a^2-b^2}}{1+\lambda} t\right] Y_{1,3}(y,0) \end{aligned}\right\} \quad (18)$$

Evaluating $Y_1(y,t)/X_1(y,t)$ and $Y_3(y,t)/X_3(y,t)$ from (18) we obtain

$$\tan\theta_{1,3}(y,t) = \frac{\sqrt{\frac{a-b}{a+b}} \sinh\left[\frac{\sqrt{a^2-b^2}}{1+\lambda} t\right] \times \cos\theta_{1,3}(y,0) + \cosh\left[\frac{\sqrt{a^2-b^2}}{1+\lambda} t\right] \sin\theta_{1,3}(y,0)}{\sqrt{\frac{a+b}{a-b}} \sinh\left[\frac{\sqrt{a^2-b^2}}{1+\lambda} t\right] \times \sin\theta_{1,3}(y,0) + \cosh\left[\frac{\sqrt{a^2-b^2}}{1+\lambda} t\right] \cos\theta_{1,3}(y,0)} \quad (19)$$

Since $\theta_1(y, 0) = \theta_3(y, 0) = \theta(y, 0)$, we have from (19)

$$\theta_1(y,t) = \theta_3(y,t) = \theta(y,t) \quad (20)$$

Evaluating $X_1(y, t)/X_3(y, t)$ or $Y_1(y, t)/Y_3(y, t)$ from (18), we obtain

$$\frac{\Psi_1}{\Psi_3}(t > 0) = \frac{\Psi_1}{\Psi_3}(t = 0) \quad (21)$$

Applying (9) to (18), we obtain (13) for $t > 0$, i.e.

$$\frac{1}{Y}\frac{\delta X}{\delta t} = \frac{1}{\Psi}\frac{\delta \Psi}{\delta t}\cot\theta - \frac{\delta\theta}{\delta t} = \frac{a+b}{1+\lambda} \quad (22\text{a})$$

$$(t > 0)$$

$$\frac{1}{X}\frac{\delta Y}{\delta t} = \frac{1}{\Psi}\frac{\delta \Psi}{\delta t}\tan\theta + \frac{\delta\theta}{\delta t} = \frac{a-b}{1+\lambda} \quad (22\text{b})$$

where a and b are defined by (14) and both are functions of y. The amplitude ratio Ψ_1/Ψ_3 is function of y only as shown by (21) and its formula is obtained from (12).

Let us call the wave given by (10) and (18) with wave properties (12), (19) and (20), and the evolution equations (22), *the characteristic wave* (cf. Holmboe, 1967). In particular, when $\delta\theta/\delta t = 0$, the product of (22a) and (22b) gives

$$\left(\frac{1}{\Psi}\frac{\delta\Psi}{\delta t}\right)^2 = \frac{a^2-b^2}{(1+\lambda)^2} \quad (\delta\theta/\delta t = 0) \quad (23)$$

With the definitions of a and b in (14), each side of (23) is precisely $(kc_i)^2$ where c_i is given by (5b). When $\delta\theta/\delta t = 0$, the ratio of (22a) to (22b) gives

$$\tan\theta_s = \sqrt{\frac{a-b}{a+b}} \quad (\delta\theta/\delta t = 0) \quad (24)$$

Therefore, the characteristic waves contain the normal mode solution. If we use the fixed conventional frame of reference given in Section 2, we have to replace x in this Section by $x - c_r t$.

4. Seasonal variation and latitudinal distribution of the quasi-geostrophic wave instability

Let us apply the normal mode solution to the real atmosphere. To do this we apply a β-plane at each reference latitude circle. By definition we have

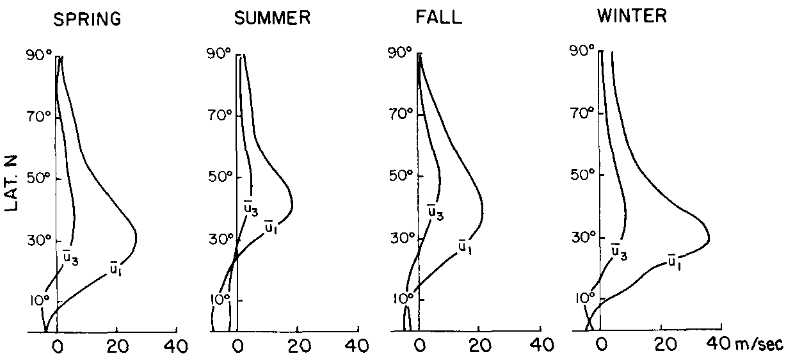

Fig. 1. The mean zonal wind at level 1 (250 mb) and at level 3 (750 mb) from the equator to north pole for the four seasons. Units: m sec^{-1}.

$$f = 2\Omega \sin \varphi \tag{25a}$$

$$\beta = 2\Omega \cos \varphi / r \tag{25b}$$

where Ω is the angular velocity of the earth's rotation, φ is the latitude and r is the radius of the earth. The wave length is

$$L = \frac{2\pi r}{m} \cos \varphi \tag{26}$$

where m is the zonal wave number. By definition we have

$$k = 2\pi/L = m/r \cos \varphi \tag{27}$$

From (27) and (25b), we get

$$\frac{\beta}{2k^2} = \frac{\Omega r}{m^2} \cos^3 \varphi \tag{28}$$

Substituting (27) and (25a) into (6c) we obtain

$$\lambda = 2(\Omega r \sin 2\varphi)^2 / S(p_2 m)^2 \tag{29}$$

The y-differential is

$$dy = r d\varphi \tag{30}$$

Substituting (28), (29) and (30) into (5a, b) we see that, given the mean zonal wind and the static stability (S), we can compute the phase speed c_r and the growth rate kc_i, for any zonal wave number m. For simplicity we shall take a constant S representing the climatological value,

$$S = 2 \times 10^{-12} \text{ m}^4 \text{ sec}^2 \text{ g}^{-2}$$

The mean zonal wind profiles are obtained from the data compiled by Oort & Rasmusson (1971) by interpolation (Fig. 1). By inspection, the strongest maximum vertical shear is at about 30° N in winter, the next strongest maximum vertical shear is in spring still at about 30° N, and the weakest maximum vertical shear is in summer at about 40° N; however, the maximum vertical shear gradually strengthens in fall at about 35° N, although it is still weak. Using the definitions of $\bar{u}_2$ and $\bar{u}_T$ given by (6a, b), we can compute $\bar{u}_2$ and $\bar{u}_T$ from $\bar{u}_1$ and $\bar{u}_3$ and then we can compute kc_i and c_r from (5a, b).

The growth rate and the phase speed for the four seasons are shown in Fig. 2. Let us consider the winter case first. We see that the maximum instability is at about 37° N, corresponding to zonal wave number 7. South of 45° N, the growth rate is stronger for zonal wave number 7 than for zonal wave number 6, but north of 45° N, the growth rate is stronger for zonal wave number 6 than for 7. Between 70° N and 80° N, the instability is a maximum for zonal wave number 4. Each of the zonal wave numbers 1 to 8 has a meridional band of instability. The stability boundaries vary with latitude such that the larger the zonal wave number, the lower the latitude of the cut-off of instability, with the exception of zonal wave number 3. For a given latitude, the phase speed is larger for larger zonal wave numbers. For individual zonal wave numbers 5 to 9, the phase speed is largest between 35° N and 40° N with the phase speed decreasing to the north and south of these latitudes except that the phase speed of zonal wave number 5

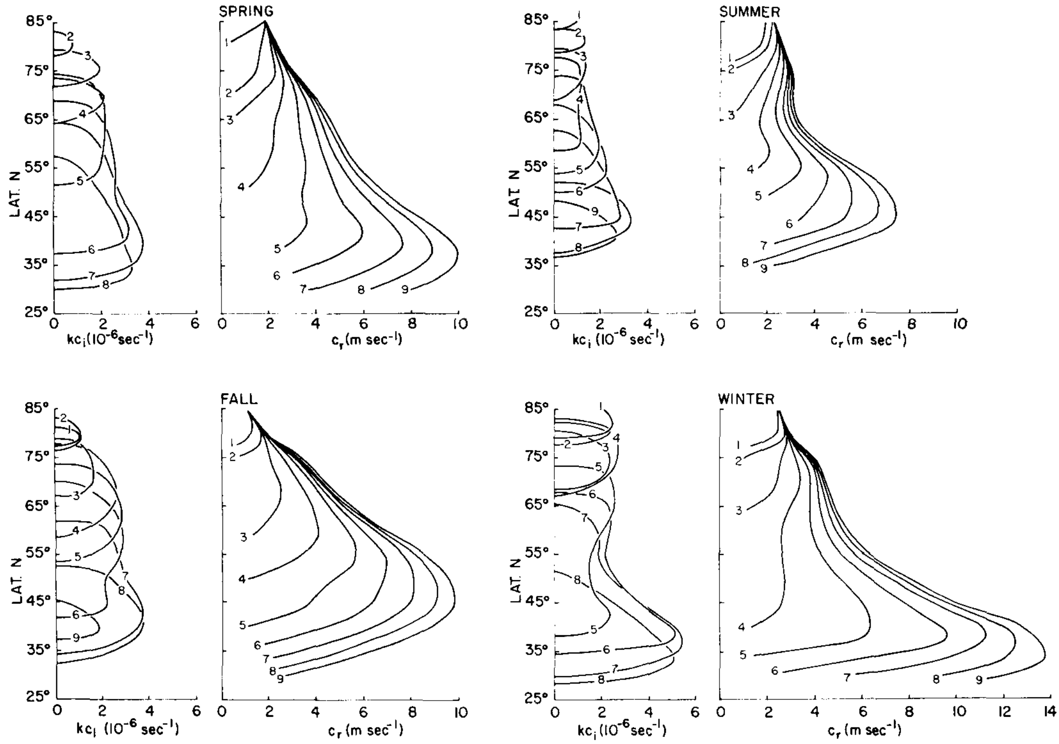

Fig. 2. The growth rate kc_i (in 10^{-6} sec^{-1}) and the phase speed c_r (in m sec^{-1}) for the four seasons for zonal wave numbers 1 to 9.

increases slightly between 65° N and 70° N. The phase speed c_r shown in the stable region is the arithmetic mean of that of the two neutral modes. The polar region is an active area of instability with zonal wave number 4 dominating between 70° N and 80° N. Near the north pole the dominant zonal wave number is one. The growth rate in summer is substantially less than that in winter for individual zonal wave numbers 1 to 4 between 70° N and 85° N. In contrast, the observations of Reed & Kunkel (1960) show a belt of high frontal wave frequency that extends along the northern shores of Siberia and the North American continent in summer (June through August 1952 to 1956) but is absent in winter. This discrepancy may be explained by the fact that in our data the vertical shear of the mean zonal wind is stronger in winter than in summer in the polar region (Fig. 1), not reflecting the strong low level thermal contrast between warm Siberian land mass and the colder Arctic air.

Next, we consider the growth rate and the phase speed for the four seasons for zonal wave numbers 6 and 7 (Fig. 3). Notice that the instability band is widest in winter, shrinks gradually in spring, is narrowest in summer, and then it expands through the fall season. The fastest growing wave shifts northward from winter through spring and summer, but then southward in fall for $m = 7$ and northward in fall for $m = 6$. In addition to the maxima in lower latitudes, there are slight maxima in the northern latitudes (winter $m = 6$, 7, spring $m = 6$) and a large maximum in the north in fall for $m = 6$. In summer there is only one maximum. These features are similar to those obtained by Phillips (1954). The right side of Fig. 3 shows the phase speeds of the waves. The fastest moving wave in all four seasons is in winter near 39° N. In spring the phase speed of the fastest moving wave is reduced, but the latitude of the fastest moving wave is at or slightly north of 40° N. In contrast, the fastest moving waves in summer and fall are in latitudes between 45 and 50° N for $m = 7$ and between 50 and 55° N for $m = 6$.

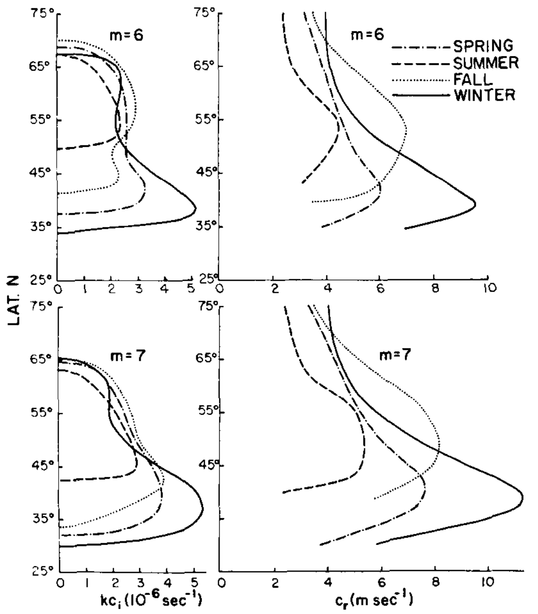

Fig. 3. The growth rate kc_i (in $10^{-6}\ \mathrm{sec}^{-1}$) and the phase speed c_r (in m sec^{-1}) in the four seasons for zonal wave numbers 6 and 7.

Next, we consider the structure of the waves. The amplitude ratio Ψ_1/Ψ_3, given by (12), and the westward tilt of the waves with height $2\theta_s$ (θ_s being given by (24)) for $m = 6$, 7 are shown in Fig. 4. Ψ_1/Ψ_3 is maximum near 50° N for summer, fall and winter, and is especially conspicuous for winter. The westward tilt of the waves with height is 5 to 8° longitude. Let us focus our attention on $m = 6$. We see that $2\theta_s$ has maxima near 60° N and near 40° N, and is a minimum near 50° N for spring, fall and winter. As mentioned at the end of Section 3, for the fixed conventional frame of reference given in Section 2, x in the formulas in Section 2 should be replaced by $x - c_r t$. Then from (10) with $\theta_1 = \theta_3 = \theta$, we can see that $2\theta_s$ is also the horizontal tilt of the wave in the upper level at $t = 0$ if we set the horizontal tilt of the wave in the lower level to zero. For $m = 6$, the waves are oriented northwest–southeast between 60° N and 50° N and northeast–southwest from 50° N to near 40° N. But as t increases, the horizontal phase difference is gradually dominated by the latitudinal variation of $c_r t$. As shown by the lines of c_r in Fig. 3, the waves are oriented northwest–southeast north of about 40° N and northeast–southwest south of it in winter and spring.

5. Conclusion

To the extent that (i) the linearized, two-level, quasi-geostrophic model is valid, (ii) the curvature of the perturbation stream function in the meridional direction can be ignored, and (iii) the sphericity of the earth can be approximated by infinite tangent β-planes, the characteristic waves with the amplitude ratio Ψ_1/Ψ_3 given by (12) have the evolutions described by (22). For a wavelength in the unstable spectrum, the asymptotic state is a growing mode whose properties were described in Section 4. The dominant zonal wave numbers are 6 and 7, especially in winter. Their seasonal variation and latitudinal distribution of the wave properties, such as the growth rate and phase speed seem to agree fairly well with the climatological distribution of cyclogenesis (cf. Petterssen, 1950). The instability is active in the polar region where the lower wave numbers dominate.

Recently Baer (1972) investigated a linearized, five-level, quasi-geostrophic model in spherical coordinates. The growth rates were comparable to ours. However, it is this author's opinion

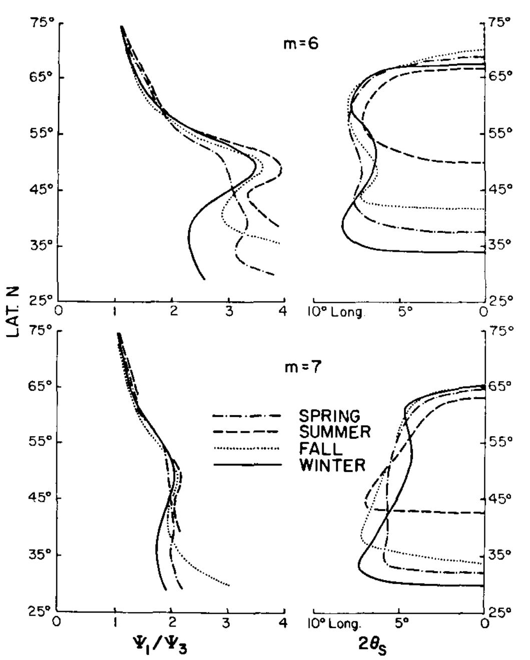

Fig. 4. The amplitude ratio, Ψ_1/Ψ_3, and the westward tilt of the wave from the level 3 to the level 1, $2\theta_s$, in the four seasons for zonal wave numbers 6 and 7.

that the special value of the present study lies in the fact that it provides a link between the theoretically more tractable β-plane models and the real atmosphere on the spherical earth.

Of course, this linearized quasi-geostrophic study has its limitations such as the exclusion of the second-order barotropic and baroclinic (nongeostrophic) effects and the dissipative mechanisms. Nevertheless, it is complimentary to studies which do consider these effects in more detail (e.g., Lipps, 1966; Saltzman & Tang, 1972).

Acknowledgements

I am deeply grateful to Professor Barry Saltzman for inspiring discussions during the course of investigation and for reading the manuscript and making useful suggestions. Some of the calculations were carried out by IBM 370/155 at Yale Computer Center with a program written by Mr Charles Levy. The manuscript was carefully typed by Mrs Linda Jensen. This research was supported by the Advanced Research Projects Agency of the Department of Defense and was monitored by U.S. Army Research Office-Durham under Grant number DA-ARO-D-31-124-71.G38.

Appendix

To test the formula for c_i as given by (5b), let us consider the parabolic jet as studied by Pedlosky (1964). The zonal wind at the upper and lower levels is, respectively,

$$\left.\begin{aligned} &\bar{u}_1 = \bar{u}^{(0)}(1-\gamma^2 y^2) \quad (-1 \leqslant \gamma y \leqslant 1) \\ &\bar{u}_3 = 0 \end{aligned}\right\} \quad \text{(A 1)}$$

Applying (A 1) to (5b), we obtain at $y=0$

$$\left[\frac{2(1+\lambda)}{\bar{u}^{(0)}}\right]^2 c_i^2 = \lambda^2 - 1 - 2(\lambda^2-\lambda-2)\left(\frac{\gamma}{k}\right)^2 - (2+\lambda)^2\left(\frac{\gamma}{k}\right)^4 - \frac{\lambda^2\beta}{k^2\bar{u}^{(0)}}\left[2\left(\frac{\gamma}{k}\right)^2 + \frac{\alpha}{k^2\bar{u}^{(0)}}\right] \quad \text{(A 2)}$$

Let us define

$$\left.\begin{aligned} &U_0 = \beta/k_0^2 \\ &k_0^2 = 2f^2/Sp_2^2 \end{aligned}\right\} \quad \text{(A 3)}$$

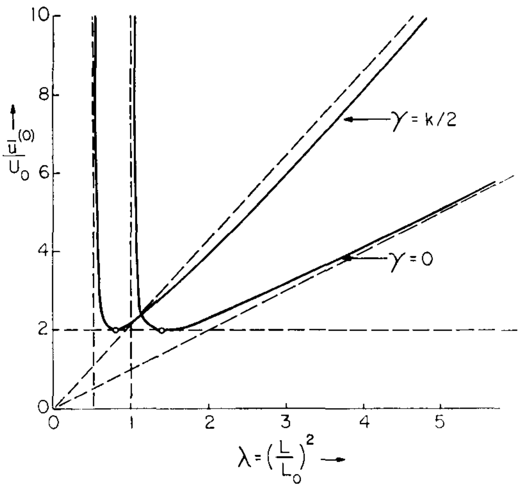

Fig. 5. The stability boundary for a parabolic jet $[\bar{u}_1 = \bar{u}^{(0)}(1-k^2y^2/4),\ \bar{u}_3 = 0]$, and that for a uniform current in y $(\bar{u}_1 = \bar{u}^{(0)},\ \bar{u}_3 = 0)$ to be compared with Pedlosky (1964, Fig. 1).

Then we have

$$\lambda = \left(\frac{k_0}{k}\right)^2 = \left(\frac{L}{L_0}\right)^2 \quad (L_0 = 2\pi/k_0) \quad \text{(A 4)}$$

In order to compare the results with those of Pedlosky (1964), let us consider the case

$$\gamma = k/2 \quad \text{(A 5)}$$

With (A 3), (A 4), and (A 5) substituted in (A 2) the stability boundary, defined by $c_i = 0$, is satisfied by

$$\bar{u}^{(0)}/U_0 = 4\lambda^2[\lambda + 2\sqrt{(\lambda+1)(2\lambda-1)}]/(7\lambda^2+4\lambda-4) \quad \text{(A 6)}$$

This has an asymptote representing a short wave cut-off at

$$\lambda = 2(2\sqrt{2}-1)/7 = 0.522 \quad (\bar{u}^{(0)} \to \infty)$$

and an asymptote representing a long wave cut-off at

$$\bar{u}^{(0)}/U_0\lambda = 4(1+2\sqrt{2})/7 = 2.188 \quad (\lambda \to \infty)$$

The stability boundary for (A 5) is shown in Fig. 5. Although the stability boundary on the long wave side appears to diverge from the asymptote, it will converge for sufficiently large wavelength and vertical zonal wind shear. For comparison, the stability boundary for $\gamma = 0$, corresponding to a mean zonal wind uniform in y in the upper layer, is also shown. The results are almost identical to those of Pedlosky (1964). The stabilizing influence of the horizontal shear of the upper-level parabolic jet on the long wave is similar to the β-effect in that the meridional gradient of the mean zonal flow is in the same direction as that of the β-gradient. The minimum vertical shear of the mean zonal wind required for instability satisfies the necessary condition for instability which states that the mean potential vorticity gradient be negative somewhere in the lower layer, i.e.

$$\beta < \bar{u}^{(0)} f^2 / S p_2^2$$

This explains why the vertical shear required for the onset of instability is the same for both cases $\gamma = k/2$ and $\gamma = 0$. However, the corresponding wavelength is shorter for the case $\gamma = k/2$ than for $\gamma = 0$ (cf. Pedlosky, 1964).

REFERENCES

Árnason, G. 1961. A study of the dynamics of a stratified fluid in relation to atmospheric motions and physical weather prediction. *Tellus 13*, 156–170.

Árnason, G. 1963. The stability of nongeostrophic perturbations in a baroclinic zonal flow. *Tellus 15*, 205–229.

Baer, F. 1972. An alternate scale representation of atmospheric energy spectra. *J. Atmos. Sci. 29*, 649–664.

Brown, J. A. 1969*a*. A numerical investigation of hydrodynamic instability and energy conversions in the quasi-geostrophic atmosphere. Part I. *J. Atmos. Sci. 26*, 352–365.

Brown, J. A. 1969*b*. A numerical investigation of hydrodynamic instability and energy conversions in the quasi-geostrophic atmosphere. Part II. *J. Atmos. Sci. 26*, 366–375.

Fleagle, R. G. 1957. On the dynamics of the general circulation. *Quart. J. Roy. Meteorol. Soc. 83*, 1–20.

Holmboe, J. 1966. The growth of a young frontal wave. *Tellus 18*, 830–837.

Holmboe, J. 1967. Dynamic properties of atmospheric motion. Part II. *Lecture Notes, Dept. Meteorology, UCLA.*

Lipps, F. B. 1966. Momentum transfer across an asymmetric jet. *J. Atmos. Sci. 23*, 213–222.

McIntyre, M. E. 1970. On the non-separable baroclinic parallel flow instability problem. *J. Fluid Mech. 40*, 273–306.

Oort, A. H. and Rasmusson, E. M. 1971. Atmospheric circulation statistics. *Professional Paper 5, NOAA*, 323 pp.

Pedlosky, J. 1964. The stability of currents in the atmosphere and the ocean. Part II. *J. Atmos. Sci. 21*, 342–353.

Pedlosky, J. 1965. On the stability of baroclinic flows as a functional of the velocity profile. *J. Atmos. Sci. 22*, 137–145.

Petterssen, S. 1950. Some aspects of the general circulation of the atmosphere. *Centenary Symposium of the General Circulation, Roy. Meteorological Soc.*, 120–155.

Phillips, N. A. 1954. Energy transformations and meridional circulations associated with simple baroclinic waves in a two-level, quasi-geostrophic model. *Tellus 6*, 273–286.

Reed, R. J. & Kunkel, B. A. 1960. The arctic circulation in summer. *J. Meteorol. 17*, 489–506.

Saltzman, B. & Tang, C.-M. 1972. Analytical study of the evolution of an amplifying baroclinic wave. *J. Atmos. Sci. 29*, 427–444.

Saltzman, B. & Vernekar, A. D. 1968. A parameterization of the large-scale transient eddy flux of relative angular momentum. *Mon. Wea. Rev. 96*, 854–857.

СЕЗОННЫЕ ИЗМЕНЕНИЯ И ШИРОТНОЕ РАСПРЕДЕЛЕНИЕ НЕУСТОЙЧИВОСТИ ДВУХУРОВЕННЫХ КВАЗИГЕОСТРОФИЗИЧЕСКИХ ВОЛН В ПОТОКЕ С ГОРИЗОНТАЛЬНЫМ СДВИГОМ

Исследуется неустойчивость упрощенной бароклинно-баротропной, двухуровенной, квазигеострофизической модели. Результаты прилагаются к описанию изменений среднего зонального ветра, который зависит от сезона и широты. Сферическая Земля аппроксимируется бесконечной касательной β-плоскостью. Найдено, что максимальная неустойчивость имеет место зимой при 37° с. ш. для волнового числа 7, изменяясь до волнового числа 6 в средних широтах и до более низких волновых чисел в полярных широтах. Широтная и спектральная полосы неустойчивости постепенно сужаются от зимы к весне, достигая минимума летом и постепенно расширяясь осенью.